PROCEEDINGS OF SCIENCE

Operation of the CMS silicon tracker

Silvia Taroni[*†]
Universitaet Zuerich
E-mail: silvia.taroni@cern.ch

The CMS silicon tracker is the largest silicon detector ever built. It consists of a hybrid pixel detector with 66 million channels and a 200 m^2 silicon strip detector with 10 million readout channels. The paper describes the operational performance of this detector during data taking years before the current LHC shutdown, during proton-proton collisions. The results here presented include signal-over-noise, hit efficiency and resolutions and effects of radiation on sensor and readout chip.

11th International Conference on Large Scale Applications and Radiation Hardness of Semiconductor Detectors
3-5 July 2013
Florence, Italy

[*]Speaker.
[†]on the behalf of the CMS collaboration

PoS(RD13)002

1. Introduction

The CMS central tracking system [1] is composed of a silicon pixel and a silicon strip tracker. Together they provide high precision measurements of charged particle trajectories in a pseudorapidity range up to $|\eta| < 2.5$.
The CMS pixel tracker has an active silicon area of $\sim$1 m^2, grouped into 1440 modules. These are arranged in three layers in the barrel region (BPIX) and two endcap disks (FPIX) on either side of the interaction point. The pixel detector uses n-in-n silicon sensors with a total of 66 million pixels of 100×150 μm^2 and a 285 μm silicon bulk providing precise 2D measurements. The CMS silicon strip tracker is the largest ever built. Its active area is almost $\sim$200 m^2 with 15148 individual silicon modules. These are arranged in 10 barrel layers and 3+9 endcap disks. In the outer parts of the silicon tracker, two silicon sensors are daisy-chained to form the silicon module. The readout pitch ranges from 80 μm in the inner layers of the inner barrel to 205 μm in the outer rings of the endcaps. The strip tracker uses p-in-n silicon with 300 (500) μm sensor thickness in the inner (outer) parts of the detector and a total of 9.6 million readout channels. In four layers (three rings) of the barrel (endcap) region, the strip tracker uses so-called stereo modules. These are modules in which two silicon sensors are mounted back-to-back with a 100 mrad stereo angle to effectively provide a 2D hit resolution also in the strip tracker. An *rz* view of one quarter of the CMS tracker is shown in figure 1. Both tracking sub-detectors of CMS are using an analog readout via optical links which retains information about the absolute signal height. The pixel detector employs an on-chip data sparsification to reduce the data volume to be shipped out. For the strip tracker all data processing is performed in the off-detector electronics.

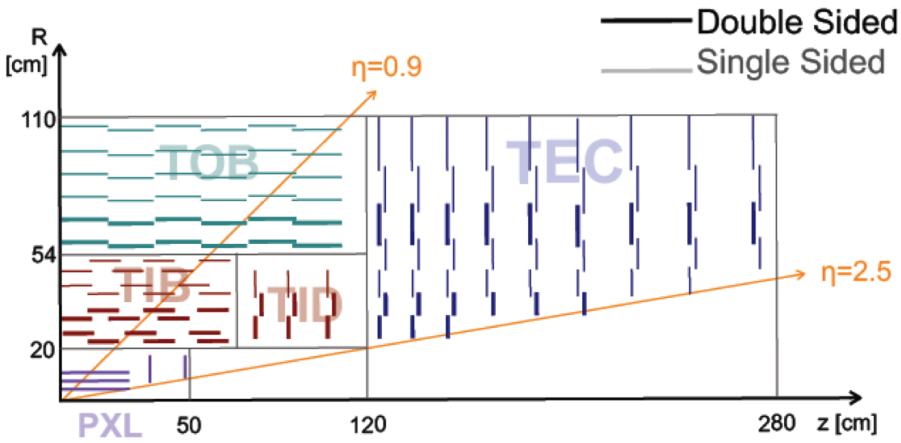

Figure 1: *rz* view of one quarter of the CMS silicon tracker. For the silicon strip tracker, layers with so-called stereo modules are drawn as thick lines.

These silicon trackers have been in more or less continuous operation during the past years of data taking. The fraction of operational channels has been reasonably constant over this period, not changing by more than a few per cent. At the end of the physics operation, the active detector fraction was about 96.3% for the pixel and 97.5% for the strip tracker. During 2012, CMS has been delivered a total of 23.3 fb^{-1} of proton - proton collision data of which 21.8 fb^{-1} have been

recorded. This corresponds to a data taking efficiency of 93.6%, higher than the 90.5% of 2011. This increase in efficiency depends on the measures implemented for operating with a doubled pile up: a more optimized trigger chain and the automatic procedures to treat the data acquisition system (DAQ) and on-detector electronic errors.

2. Pixel detector

The pixel detector is working successfully since its installation in 2008. During 2012, pixel operational issues accounted for only 9% of CMS downtime. Only 3.7% of the Read-Out Chips (ROCs) are unavailable for readout; the major type of lost channels is ROC producing an incorrect pulse shape, which results in the signal being unidentified within the analog pulse train. One entire optical channel in the FPIX is lost due to a broken laser driver. Most of these unavailable channels are going to be recovered in the current LHC shutdown.

2.1 Hit efficiency and resolution

Pixel hit efficiencies are determined by measuring missing hits on reconstructed tracks during LHC running. The efficiency for working ROCs is above 99% for all layers, as shown in figure 2. However, the module hit efficiency decreases as function of the instantaneous luminosity, as shown in figure 3, with the pixel modules in the innermost layer of the BPIX, layer 1, being affected the most. This is mainly caused by a dynamic inefficiency which increases with hit rate and originates from limitations in the internal buffering of the readout chip [2].

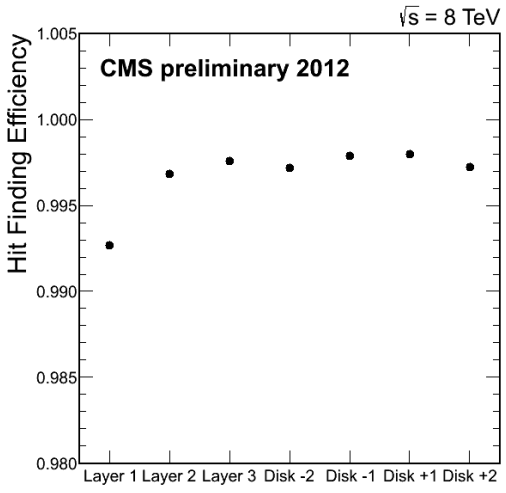

Figure 2: Hit finding efficiency as function of layer for the pixel detector.

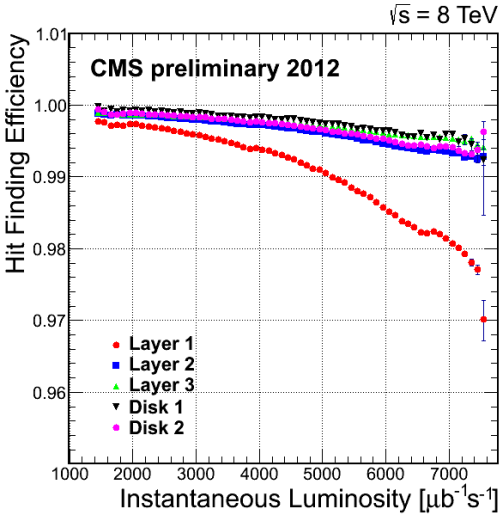

Figure 3: Hit finding efficiency dependence on the instantaneous luminosity.

Despite this loss in efficiency, the pixel detector is performing well in terms of resolution. The hit resolutions are measured using the triplet method, in which tracks with 3 hits in the barrel are extrapolated to layer 2 using the layer 1 and 3 positions and angles. The residual in both ϕ and z direction may then be measured: they are shown in figure 4 and 5.

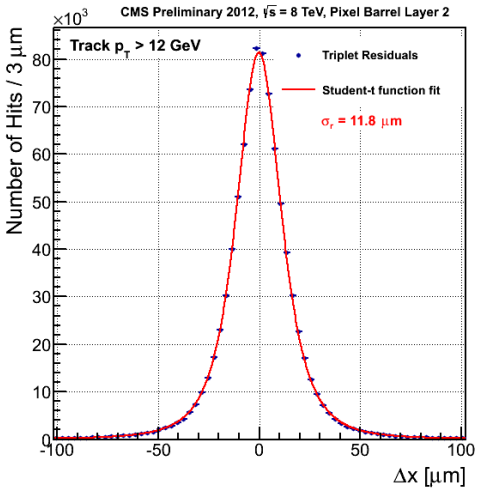

Figure 4: Hit resolution in ϕ direction obtained from the triplet method.

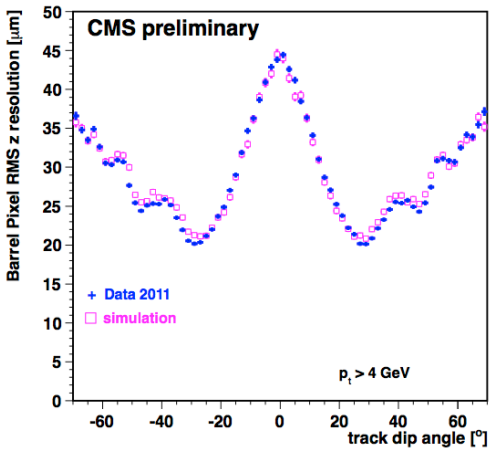

Figure 5: Resolution in the z direction as a function of the track incidence angle.

2.2 Effects of radiation

The CMS pixel detector has been designed to be able to continue operation even after significant radiation damage. Nevertheless, there is the need to monitor the damage through studies of the leakage current and depletion voltage evolution.

The depletion voltage is investigated by varying the bias voltage at which the detector is operated during the LHC operation and thus changing the charge collection and hit efficiency. The hit efficiency measurement during a bias scan for layer 1 is shown in figure 6. The dependence of the voltage needed to have the 99% efficiency on the total integrated luminosity is shown in figure 7 where a minimum at 8-10 fb^{-1} of integrated luminosity is clearly visible: layer 1 has been type inverted during 2012 data taking.

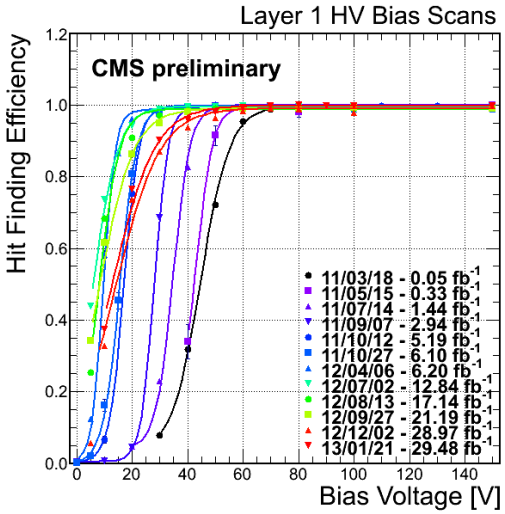

Figure 6: Hit efficiency results from the bias scan, taken at various luminosities, for layer 1.

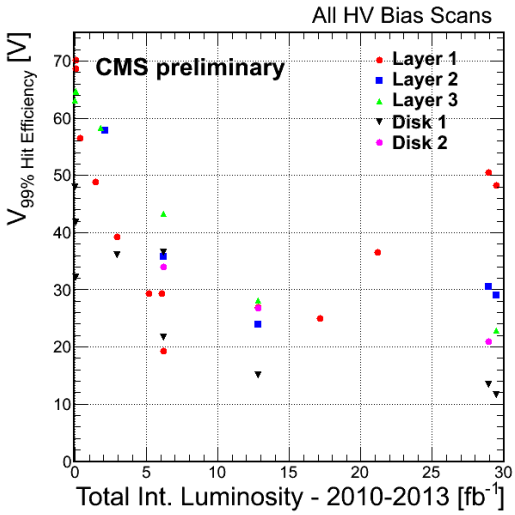

Figure 7: Voltage for which the hit efficiency is 99% at different integrated luminosities and for different layers. The points at 0 fb^{-1} for layer 1, 3, and disk 1 have been taken during the 2010 run (total integrated luminosity 44.2 pb^{-1}). The two points at 6 fb^{-1} has been taken at the end of the 2011 and at the beginning of the 2012. Layer 1 points (red dots) clearly show a minimum at 8-10 fb^{-1}: it has been type inverted during 2012 data taking.

Leakage current is measured in the pixel barrel, using readings from the high voltage power supplies, and compared to models of leakage current evolution in radiation damage. In order to facilitate comparison between experiments, measured leakage currents are normalized by the area of instrumented silicon and extrapolated to 0°C [3].
The leakage current averaged over each barrel layer is shown in figure 8 and 9, as a function of integrated luminosity and of time in 2011-12. The data are compared to a parameterization adding exponential and logarithmic terms [4], which accounts for accumulated damage and for annealing, whose input is the fluence as predicted by a model of the CMS detector implemented in the FLUKA program [5, 6]. This model produced good agreement in shape with data but needed to

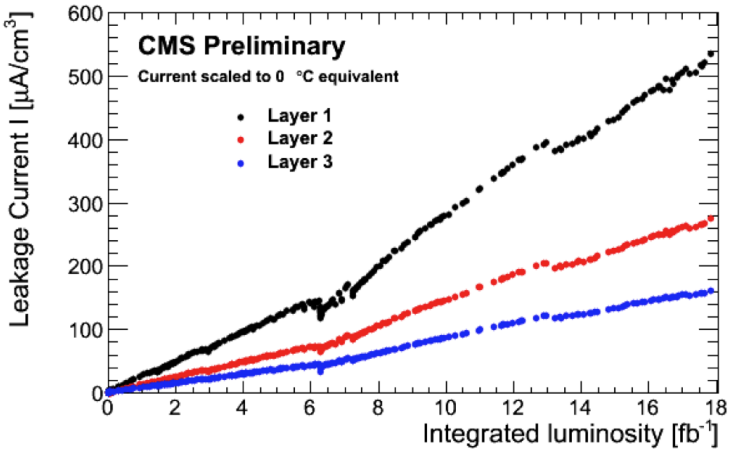

Figure 8: Average leakage current in each barrel layer as a function of integrated luminosity.

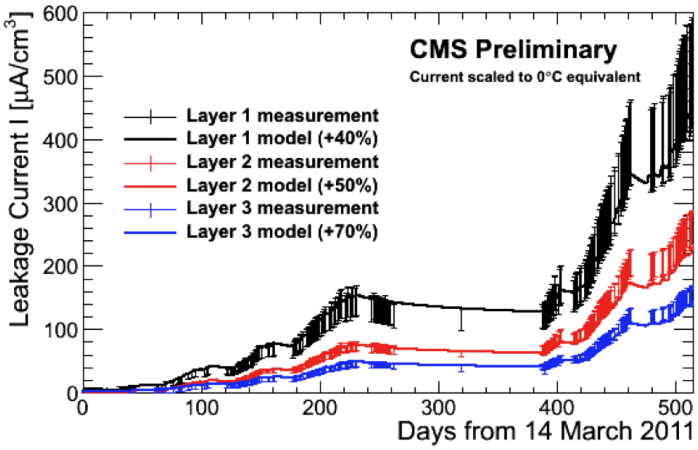

Figure 9: Average leakage current in each barrel layer as a function of time in 2011 and 2012.

be rescaled. The reason for these discrepancies in scale are under investigation, with possibilities including uncertainties in the operational temperature of the detector.
During the 2012 running, it has been observed that the analog current drawn increases with time, necessitating analog recalibration in order to avoid exceeding power supply limits. This effect was not anticipated. A possible explanation is that it derives from bulk damage in the diode used as a reference voltage within the ROC. Same reason has been guessed for the pixel threshold increase that have been observed in the data taking (figure 10) and that has required optimization to not affect the data quality.

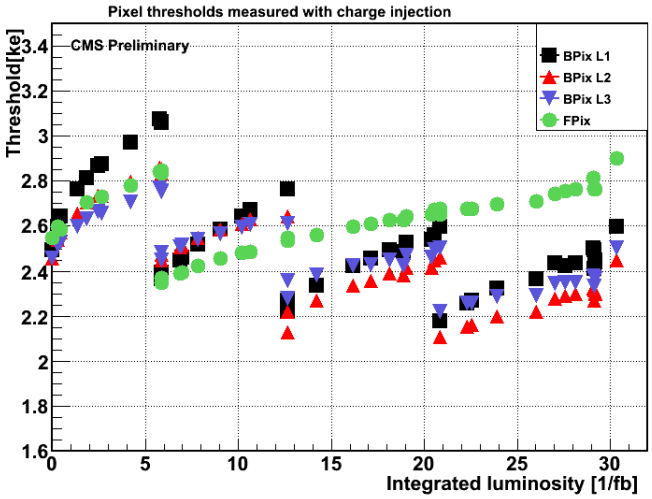

Figure 10: Pixel threshold trend in 2011 and 2012 as function of the integrated luminosity. Optimizations were performed for the whole detector at the end of 2011 run (~ 6 fb^{-1}) and for barrel layers only in 2012.

Because of the harsh environment where the pixel detector lives, bit flips caused by Single Event Upsets may occur in electronics at the pixel, ROC or higher-level on-detector electronics that controls many ROCs. In this last case, a significant part of the detector may become non-operational

until a reset. During 2012, this happened, on average, every 73 pb^{-1} of data. To avoid the loss of data and quality degradation, techniques for detection and recovery have been implemented in the pixel software. If a readout channel does not return data, or if too many synchronization errors are observed, the CMS central trigger is stopped automatically, all detector electronics at the ROC level and above is reprogrammed and the data taking is resumed in few seconds.

3. Strip Detector

The strip detector operated well during the past data taking with only ∼2.5% of the modules excluded because of problems with high voltage short circuits, control rings failures or other issues.

3.1 Signal-to-noise ratio, hit efficiency and resolution

The first step towards high quality tracking data is the efficient and accurate reconstruction of hits from crossing particles. In figure 11 and figure 12 an example from the strip tracker of the signal-to-noise ratio for hits on reconstructed tracks is shown. The ratio is evaluated on the basis of charge clusters associated with reconstructed tracks, where the individual strip noise values are taken from calibration runs. For track angles that are not normal to the surface of modules the signal values are corrected to compensate for the different path length. Cluster noise, which takes into account the noise of each strip within a cluster, is used as the denominator in the S/N ratio. A fit to the distribution with a Landau distribution convoluted with a Gaussian yields a most probable value (MPV) of 18.4 for the inner barrel (TIB) and 22.4 for the outer barrel (TOB). The tracker inner disk (TID) and the tracker endcap (TEC) S/N varies between 19.2 and 26.1 [8]; these values reflect the different sensor thickness, strip length and pitch and allow for an efficient hit reconstruction.

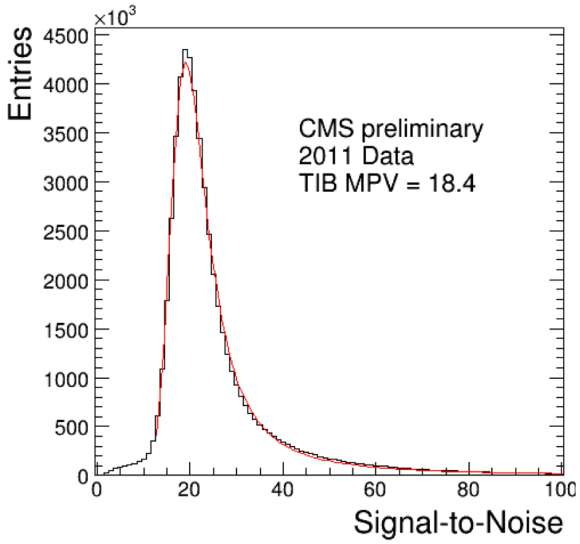

Figure 11: Signal-to-noise distribution from hits on reconstructed particle tracks in TIB.

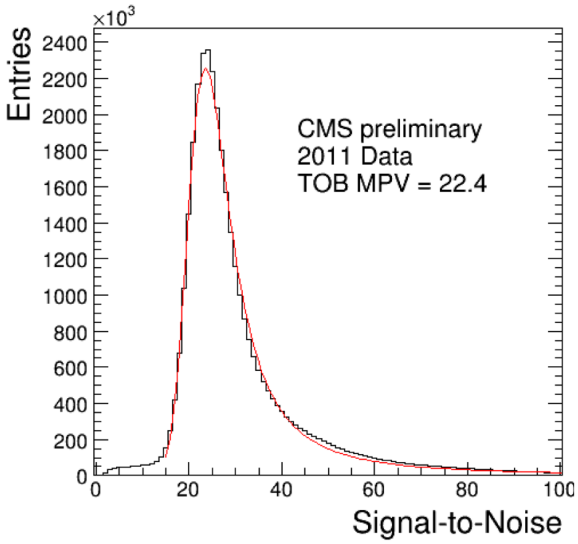

Figure 12: Signal-to-noise distribution from hits on reconstructed particle tracks in TIB.

The hit efficiency has been measured requiring tracks having a minimum of 8 hits. To avoid inactive regions and allow for alignment imprecision, trajectories passing near the edges of sensors

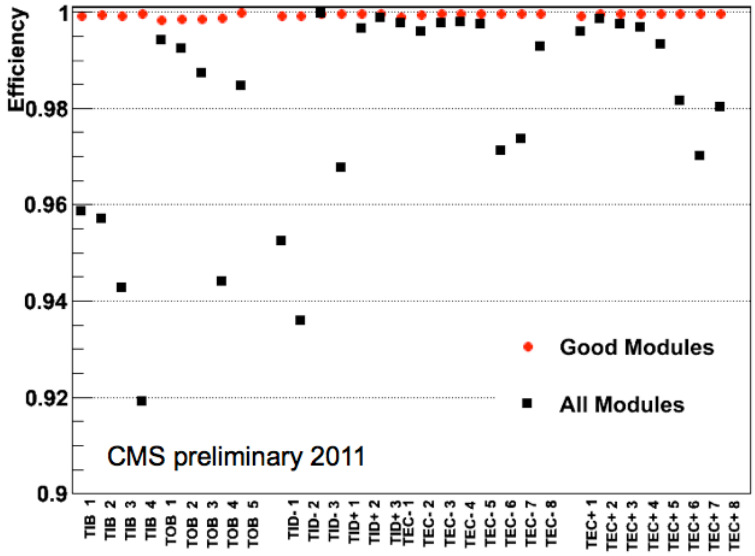

Figure 13: Single hit efficiencies of the strip tracker measured from data.

were excluded. The presence of a hit anywhere within the non-excluded region of a traversed module was counted as a positive response; efficiency is determined by the ratio of positive responses to the total number of traversing tracks. In figure 13 the resulting hit efficiency is shown for two cases. In black, the efficiency is shown in case one assumes a perfect detector without any non-functional modules. In red, the hit efficiency is shown when taking into account known inefficient regions. One can see that in this second case, the hit efficiency is about 99.8% in all detector parts, consistent with the $\sim 0.2\%$ of bad channel estimated by the module quality control tests during the production.

The resolution of the reconstructed hit positions on the modules has been measured using tracks with two hits in one layer, i.e. in the overlap regions of the modules [7]. The employed double-difference technique is largely insensitive to misalignment effects and multiple scattering.The difference of the reconstructed hits from predictions, fitted to a Gaussian function, provides a hit resolution convoluted with the uncertainty from the trajectory propagation. As the two overlapping modules are expected to have the same resolution, the resolution of a single sensor is determined by dividing the standard deviation by $\sqrt{2}$. The measurement has been performed for the inner barrel (TIB) and outer barrel (TOB): the hit resolution varies between 15.5 and 41.3 μm, with a strong dependence on strip pitch.

3.2 Radiation Monitoring

During the two years 2011 and 2012, the silicon detectors acquired a radiation dose corresponding to 29.4 fb^{-1}. The effects of irradiation are closely monitored by performing various scans of the radiation related quantities. For the depletion voltage two types of scans are performed regularly. One is using tracks from p-p collisions to study the signal dependence on bias voltage whereas the other relies on random triggers during periods without beam to investigate the noise

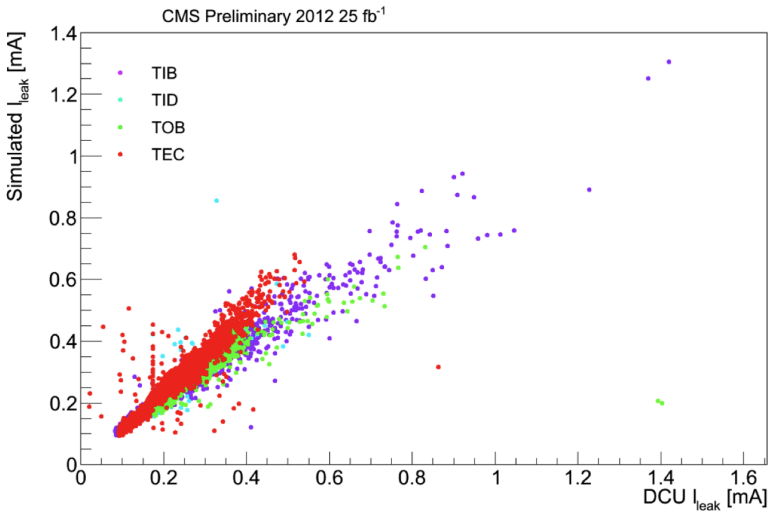

Figure 14: Plot of the leakage current compared with simulation. Results are corrected for module type, radius and sensor temperature.

behavior. At least once per month, a small scan of the bias voltage with p-p collisions is performed. For this, a set of representative power groups from different parts of the tracker is scanned.
For the leakage current, measurements are performed using both in-situ measurements from the detector control units (DCUs) on each module and current measurements from the power supply units. In the latter, the measured current corresponds to several detector modules (3-12) due to the limited granularity of the power system. Both methods provide consistent results.
In figure 14, the measured leakage current is compared to a prediction from FLUKA simulation. One can see that there is good agreement between the simulation and the data.

4. Conclusions

The CMS full silicon tracker operated successfully in the whole data taking period. Only few channels are lost because of problems in readout chain, control rings or high voltage short circuits. The hit efficiency and resolution are anyway excellent. The effect of radiation is continuously monitored and compared to models; studies are ongoing to understand the discrepancies. Automatic procedures have been developed to mitigate the effects of SEU.

References

[1] S. Chatrchyan et al. [CMS Collaboration], "The CMS experiment at the CERN LHC", JINST 3 (2008) S08004.

[2] CMS Collaboration, "CMS technical design report for the pixel detector upgrade", CERN, Geneva, Tech. Rep. CERN-LHCC-2012-016. CMS-TDR-011, Sep 2012. Available online at: http://cdsweb.cern.ch/ record/1481838.

[3] S. M. Sze, "Semiconductor Devices: Physics and Technology", New York, Wiley, 1985.

[4] M. Moll, Ph.D thesis, University of Hamburg (1999), DESY-THESIS-1999-040.

[5] A. Ferrari, P. R. Sala, A. Fasso and J. Ranft, "FLUKA: A multi-particle transport code (Program version 2005)", CERN-2005-010.

[6] G. Battistoni, S. Muraro, P. R. Sala, F. Cerutti, A. Ferrari, S. Roesler, A. Fasso and J. Ranft, "The FLUKA code: Description and benchmarking", AIP Conf. Proc. 896 (2007) 31.

[7] CMS Tracker Collaboration, "Stand-Alone Cosmic Muon Reconstruction before Installation of the CMS Silicon Strip Tracker", JINST 4 (2009) P05004

[8] V. Khachatryan et al. [CMS Collaboration], "Tracking Performance Results from early LHC Operation", Eur. Phys. J. C 70, 1165 (2010)